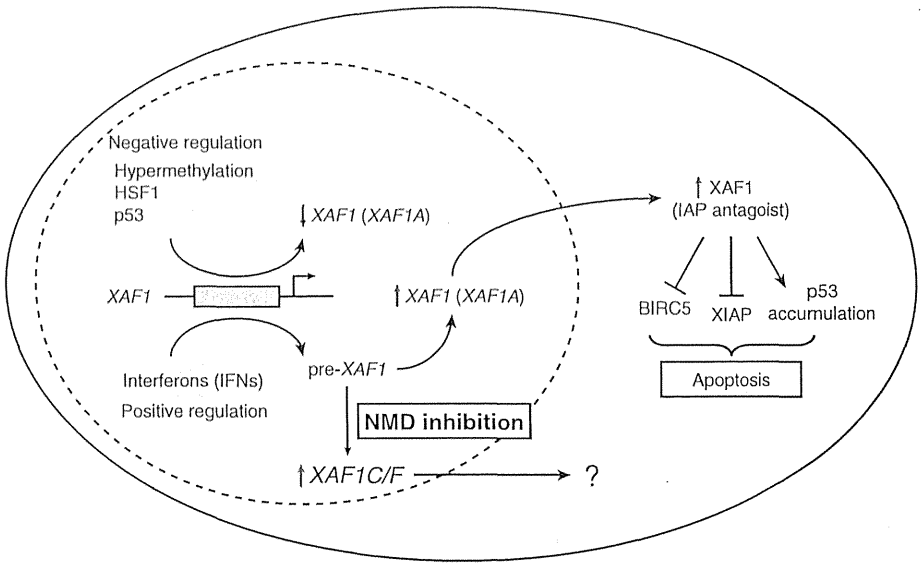

Fig. 6 Key roles of XAF1 in cancer cells. The transcription of the *XAF1* gene is under the control of negative and positive regulatory elements. NMD inhibition promotes accumulation of *XAF1F*. *Gray arrows* indicate the upregulation or downregulation of the *XAF1* transcripts. HSF and XIAP represent heat shock factor 1 and XIAP, respectively

Fisher's exact test). In stage I and II, 67 % (2/3) and 90 % (9/10) of patients with lymph node metastasis were categorized as *XAF1F* positive, respectively. These results suggest that *XAF1F* expression in CTCs strongly reflects lymph node metastasis in stage I and II, leading to a weak association between *XAF1F* expression and tumor stage. Additionally, *XAF1F* expression in CTCs was not associated with recurrence, although CTCs are useful as a prognostic factor [36, 44–47]. In further studies, this discrepancy should be also examined using long-term follow-up data of CTCs isolated from patients to clarify the origin of the *XAF1* variant.

In conclusion, the present study identified a novel splice variant of *XAF1* in gastric, pancreatic, colorectal, and breast cancer cells. This variant was regulated through the NMD pathway and accumulated in NMD-suppressed metastatic cancer cells. To our knowledge, this is the first study to clearly detect *XAF1* variants in peripheral blood containing CTCs derived from gastric cancer. The expression of these variants was significantly higher than that in healthy volunteers. Furthermore, in part of the CTC-positive population, the NMD pathway was suppressed. These findings suggest that *XAF1* variants accumulate by NMD inhibition in the peripheral blood of gastric cancer patients and may indicate heterogeneity of CTCs.

Acknowledgments This research was supported by a Grant-in-Cooperation of the Regional Innovation Cluster Program 2010 and Japan Society for the Promotion of Science KAKENHI 23701092 and 25710013. The authors thank Yuko Watanabe, Kaori Kanto, and Tomomi Ide for their technical assistance, Keita Mori for statistical advice, and Dr. Takashi Sugino for comments on the clinicopathological data.

Conflict of interest The authors have no conflict of interest.

References

1. Liston P, Fong WG, Kelly NL, et al. Identification of XAF1 as an antagonist of XIAP anti-caspase activity. Nat Cell Biol. 2001;3(2):128–33.
2. Byun DS, Cho K, Ryu BK, et al. Hypermethylation of XIAP-associated factor 1, a putative tumor suppressor gene from the 17p13.2 locus, in human gastric adenocarcinomas. Cancer Res. 2003;63(21):7068–75.
3. Arora V, Cheung HH, Plenchette S, et al. Degradation of survivin by the X-linked inhibitor of apoptosis (XIAP)-XAF1 complex. J Biol Chem. 2007;282(36):26202–9.
4. Tu SP, Liston P, Cui JT, et al. Restoration of XAF1 expression induces apoptosis and inhibits tumor growth in gastric cancer. Int J Cancer. 2009;125(3):688–97.
5. Huang J, Yao WY, Zhu Q, et al. XAF1 as a prognostic biomarker and therapeutic target in pancreatic cancer. Cancer Sci. 2010;101(2):559–67.
6. Sun PH, Zhu LM, Qiao MM, et al. The XAF1 tumor suppressor induces autophagic cell death via upregulation of Beclin-1 and inhibition of Akt pathway. Cancer Lett. 2011;310(2):170–80.
7. Zou B, Chim CS, Pang R, et al. XIAP-associated factor 1 (XAF1), a novel target of p53, enhances p53-mediated apoptosis via post-translational modification. Mol Carcinog. 2012;51(5):422–32.
8. Fong WG, Liston P, Rajcan-Separovic E, et al. Expression and genetic analysis of XIAP-associated factor 1 (XAF1) in cancer cell lines. Genomics. 2000;70(1):113–22.
9. Zou B, Chim CS, Zeng H, et al. Correlation between the single-site CpG methylation and expression silencing of the XAF1 gene in human gastric and colon cancers. Gastroenterology. 2006;131(6):1835–43.
10. Lee MG, Huh JS, Chung SK, et al. Promoter CpG hypermethylation and downregulation of XAF1 expression in human urogenital malignancies: implication for attenuated p53 response to apoptotic stresses. Oncogene. 2006;25(42):5807–22.
11. Yin W, Cheepala S, Clifford JL. Identification of a novel splice variant of X-linked inhibitor of apoptosis-associated factor 1. Biochem Biophys Res Commun. 2006;339(4):1148–54.
12. Chung SK, Lee MG, Ryu BK, et al. Frequent alteration of XAF1 in human colorectal cancers: implication for tumor cell resistance to apoptotic stresses. Gastroenterology. 2007;132(7):2459–77.

13. Plenchette S, Cheung HH, Fong WG, et al. The role of XAF1 in cancer. Curr Opin Invest Drugs. 2007;8(6):469–76.
14. Fang X, Liu Z, Fan Y, et al. Switch to full-length of XAF1 mRNA expression in prostate cancer cells by the DNA methylation inhibitor. Int J Cancer. 2006;118(10):2485–9.
15. Maquat LE. Nonsense-mediated mRNA decay. Curr Biol. 2002;12(6):R196–7.
16. Mendell JT, Sharifi NA, Meyers JL, et al. Nonsense surveillance regulates expression of diverse classes of mammalian transcripts and mutes genomic noise. Nat Genet. 2004;36(10):1073–8.
17. Gardner LB. Nonsense-mediated RNA decay regulation by cellular stress: implications for tumorigenesis. Mol Cancer Res. 2010;8(3):295–308.
18. Gardner LB. Hypoxic inhibition of nonsense-mediated RNA decay regulates gene expression and the integrated stress response. Mol Cell Biol. 2008;28(11):3729–41.
19. Wang D, Zavadil J, Martin L, et al. Inhibition of nonsense-mediated RNA decay by the tumor microenvironment promotes tumorigenesis. Mol Cell Biol. 2011;31(17):3670–80.
20. Tani H, Torimura M, Akimitsu N. The RNA degradation pathway regulates the function of GAS5 a non-coding RNA in mammalian cells. PLoS One. 2013;8(1):e55684.
21. Wang S, Zheng G, Cheng B, et al. Circulating tumor cells (CTCs) detected by RT-PCR and its prognostic role in gastric cancer: a meta-analysis of published literature. PLoS One. 2014;9(6):e99259.
22. Powell AA, Talasaz AH, Zhang H, et al. Single cell profiling of circulating tumor cells: transcriptional heterogeneity and diversity from breast cancer cell lines. PLoS One. 2012;7(5):e33788.
23. Neuert G, Munsky B, Tan RZ, et al. Systematic identification of signal-activated stochastic gene regulation. Science. 2013;339(6119):584–7.
24. Zhang ZY, Ge HY. Micrometastasis in gastric cancer. Cancer Lett. 2013;336(1):34–45.
25. Savagner P, Valles AM, Jouanneau J, et al. Alternative splicing in fibroblast growth factor receptor 2 is associated with induced epithelial-mesenchymal transition in rat bladder carcinoma cells. Mol Biol Cell. 1994;5(8):851–62.
26. Pino MS, Balsamo M, Di Modugno F, et al. Human Mena+11a isoform serves as a marker of epithelial phenotype and sensitivity to epidermal growth factor receptor inhibition in human pancreatic cancer cell lines. Clin Cancer Res. 2008;14(15):4943–50.
27. Warzecha CC, Sato TK, Nabet B, et al. ESRP1 and ESRP2 are epithelial cell-type-specific regulators of FGFR2 splicing. Mol Cell. 2009;33(5):591–601.
28. Shapiro IM, Cheng AW, Flytzanis NC, et al. An EMT-driven alternative splicing program occurs in human breast cancer and modulates cellular phenotype. PLoS Genet. 2011;7(8):e1002218.
29. Valacca C, Bonomi S, Buratti E, et al. Sam68 regulates EMT through alternative splicing-activated nonsense-mediated mRNA decay of the SF2/ASF proto-oncogene. J Cell Biol. 2010;191(1):87–99.
30. Fujita Y, Terashima M, Hoshino Y, et al. Detection of cancer cells disseminated in bone marrow using real-time quantitative RT-PCR of CEA, CK19, and CK20 mRNA in patients with gastric cancer. Gastric Cancer. 2006;9(4):308–14.
31. Huang P, Wang J, Guo Y, et al. Molecular detection of disseminated tumor cells in the peripheral blood in patients with gastrointestinal cancer. J Cancer Res Clin Oncol. 2003;129(3):192–8.
32. Ishigami S, Sakamoto A, Uenosono Y, et al. Carcinoembryonic antigen messenger RNA expression in blood can predict relapse in gastric cancer. J Surg Res. 2008;148(2):205–9.
33. Helo P, Cronin AM, Danila DC, et al. Circulating prostate tumor cells detected by reverse transcription-PCR in men with localized or castration-refractory prostate cancer: concordance with Cell Search assay and association with bone metastases and with survival. Clin Chem. 2009;55(4):765–73.
34. Danila DC, Anand A, Schultz N, et al. Analytic and clinical validation of a prostate cancer-enhanced messenger RNA detection assay in whole blood as a prognostic biomarker for survival. Eur Urol 2014;65(6):1191–7
35. Cao W, Yang W, Li H, et al. Using detection of survivin-expressing circulating tumor cells in peripheral blood to predict tumor recurrence following curative resection of gastric cancer. J Surg Oncol. 2011;103(2):110–5.
36. Cao M, Yie SM, Wu SM, et al. Detection of survivin-expressing circulating cancer cells in the peripheral blood of patients with esophageal squamous cell carcinoma and its clinical significance. Clin Exp Metastasis. 2009;26(7):751–8.
37. Ivanov I, Lo KC, Hawthorn L, et al. Identifying candidate colon cancer tumor suppressor genes using inhibition of nonsense-mediated mRNA decay in colon cancer cells. Oncogene. 2007;26(20):2873–84.
38. Robin X, Turck N, Hainard A, et al. pROC: an open-source package for R and S+ to analyze and compare ROC curves. BMC Bioinform. 2011;12:77.
39. Xia J, Broadhurst DI, Wilson M, et al. Translational biomarker discovery in clinical metabolomics: an introductory tutorial. Metabolomics. 2013;9(2):280–99.
40. Huang L, Lou CH, Chan W, et al. RNA homeostasis governed by cell type-specific and branched feedback loops acting on NMD. Mol Cell. 2011;43(6):950–61.
41. Chan WK, Huang L, Gudikote JP, et al. An alternative branch of the nonsense-mediated decay pathway. EMBO J. 2007;26(7):1820–30.
42. Schroeder A, Mueller O, Stocker S, et al. The RIN: an RNA integrity number for assigning integrity values to RNA measurements. BMC Mol Biol. 2006;7:3.
43. Bruning O, Rodenburg W, Radonic T, et al. RNA isolation for transcriptomics of human and mouse small skin biopsies. BMC Res Notes. 2011;4:438.
44. Yie SM, Lou B, Ye SR, et al. Detection of survivin-expressing circulating cancer cells (CCCs) in peripheral blood of patients with gastric and colorectal cancer reveals high risks of relapse. Ann Surg Oncol. 2008;15(11):3073–82.
45. Bertazza L, Mocellin S, Marchet A, et al. Survivin gene levels in the peripheral blood of patients with gastric cancer independently predict survival. J Transl Med. 2009;7:111.
46. Hoffmann AC, Warnecke-Eberz U, Luebke T, et al. Survivin mRNA in peripheral blood is frequently detected and significantly decreased following resection of gastrointestinal cancers. J Surg Oncol. 2007;95(1):51–4.
47. Terashima M, Yamakawa Y, Hatakeyama K, et al. Survivin expression in peripheral blood as a prognostic marker in patients with gastric cancer. J Clin Oncol 2014;32(suppl 15).
48. Black DL. Mechanisms of alternative pre-messenger RNA splicing. Annu Rev Biochem. 2003;72:291–336.
49. Birney E, Andrews D, Bevan P, et al. Ensembl 2004. Nucleic Acids Res 2004;32(database issue):D468–D470.
50. Birney E, Andrews TD, Bevan P, et al. An overview of Ensembl. Genome Res. 2004;14(5):925–8.
51. Furuta K, Arao T, Sakai K, et al. Integrated analysis of whole genome exon array and array-comparative genomic hybridization in gastric and colorectal cancer cells. Cancer Sci. 2012;103(2):221–7.
52. Hatakeyama K, Ohshima K, Fukuda Y, et al. Identification of a novel protein isoform derived from cancer-related splicing variants using combined analysis of transcriptome and proteome. Proteomics. 2011;11(11):2275–82.
53. Pastor F, Kolonias D, Giangrande PH, et al. Induction of tumour immunity by targeted inhibition of nonsense-mediated mRNA decay. Nature (Lond). 2010;465(7295):227–30.

54. Bonomi S, di Matteo A, Buratti E, et al. HnRNP A1 controls a splicing regulatory circuit promoting mesenchymal-to-epithelial transition. Nucleic Acids Res. 2013;41(18):8665–79.
55. Garcia-Olmo DC, Ruiz-Piqueras R, Garcia-Olmo D. Circulating nucleic acids in plasma and serum (CNAPS) and its relation to stem cells and cancer metastasis: state of the issue. Histol Histopathol. 2004;19(2):575–83.
56. Valadi H, Ekstrom K, Bossios A, et al. Exosome-mediated transfer of mRNAs and microRNAs is a novel mechanism of genetic exchange between cells. Nat Cell Biol. 2007;9(6):654–9.
57. Ohshima K, Inoue K, Fujiwara A, et al. Let-7 microRNA family is selectively secreted into the extracellular environment via exosomes in a metastatic gastric cancer cell line. PLoS One. 2010;5(10):e13247.
58. Meng S, Tripathy D, Shete S, et al. HER-2 gene amplification can be acquired as breast cancer progresses. Proc Natl Acad Sci USA. 2004;101(25):9393–8.
59. Gradilone A, Petracca A, Nicolazzo C, et al. Prognostic significance of survivin-expressing circulating tumour cells in T1G3 bladder cancer. BJU Int. 2010;106(5):710–5.
60. Krebs MG, Hou JM, Sloane R, et al. Analysis of circulating tumor cells in patients with non-small cell lung cancer using epithelial marker-dependent and -independent approaches. J Thorac Oncol. 2012;7(2):306–15.
61. Zhao L, Li P, Li F, et al. The prognostic value of circulating tumor cells lacking cytokeratins in metastatic breast cancer patients. J Cancer Res Ther. 2013;9(1):29–37.
62. Hosokawa M, Kenmotsu H, Koh Y, et al. Size-based isolation of circulating tumor cells in lung cancer patients using a microcavity array system. PLoS One. 2013;8(6):e67466.
63. Wang J, He H, Yu L, et al. HSF1 down-regulates XAF1 through transcriptional regulation. J Biol Chem. 2006;281(5):2451–9.
64. Zhang W, Guo Z, Jiang B, et al. Identification of a functional p53 responsive element within the promoter of XAF1 gene in gastrointestinal cancer cells. Int J Oncol. 2010;36(4):1031–7.
65. Leaman DW, Chawla-Sarkar M, Vyas K, et al. Identification of X-linked inhibitor of apoptosis-associated factor-1 as an interferon-stimulated gene that augments TRAIL Apo2L-induced apoptosis. J Biol Chem. 2002;277(32):28504–11.
66. Chawla-Sarkar M, Lindner DJ, Liu YF, et al. Apoptosis and interferons: role of interferon-stimulated genes as mediators of apoptosis. Apoptosis. 2003;8(3):237–49.
67. Wang J, Peng Y, Sun YW, et al. All-trans retinoic acid induces XAF1 expression through an interferon regulatory factor-1 element in colon cancer. Gastroenterology. 2006;130(3):747–58.
68. Micali OC, Cheung HH, Plenchette S, et al. Silencing of the XAF1 gene by promoter hypermethylation in cancer cells and reactivation to TRAIL-sensitization by IFN-beta. BMC Cancer. 2007;7:52.
69. Reu FJ, Bae SI, Cherkassky L, et al. Overcoming resistance to interferon-induced apoptosis of renal carcinoma and melanoma cells by DNA demethylation. J Clin Oncol. 2006;24(23):3771–9.
70. Mitchell MJ, King MR. Computational and experimental models of cancer cell response to fluid shear stress. Front Oncol. 2013;3:44.
71. Gakhar G, Navarro VN, Jurish M, et al. Circulating tumor cells from prostate cancer patients interact with E-selectin under physiologic blood flow. PLoS One. 2013;8(12):e85143.
72. Kutun S, Celik A, Cem Kockar M, et al. Expression of CK-19 and CEA mRNA in peripheral blood of gastric cancer patients. Exp Oncol. 2010;32(4):263–8.
73. Schulze K, Gasch C, Staufer K, et al. Presence of EpCAM-positive circulating tumor cells as biomarker for systemic disease strongly correlates to survival in patients with hepatocellular carcinoma. Int J Cancer. 2013;133(9):2165–71.
74. Partridge M, Brakenhoff R, Phillips E, et al. Detection of rare disseminated tumor cells identifies head and neck cancer patients at risk of treatment failure. Clin Cancer Res. 2003;9(14):5287–94.
75. Hristozova T, Konschak R, Stromberger C, et al. The presence of circulating tumor cells (CTCs) correlates with lymph node metastasis in nonresectable squamous cell carcinoma of the head and neck region (SCCHN). Ann Oncol. 2011;22(8):1878–85.
76. Tsuji T, Ibaragi S, Hu GF. Epithelial-mesenchymal transition and cell cooperativity in metastasis. Cancer Res. 2009;69(18):7135–9.

Gastric Cancer
DOI 10.1007/s10120-014-0424-5

SHORT COMMUNICATION

Anatomical considerations of the infrapyloric artery and its associated lymph nodes during laparoscopic gastric cancer surgery

Shusuke Haruta · Hisashi Shinohara · Masaki Ueno · Harushi Udagawa · Yoshiharu Sakai · Ichiro Uyama

Received: 27 May 2014 / Accepted: 23 August 2014

Abstract
Background Little is known about the vascular and lymphatic distribution of the pyloric antrum in the stomach. We focused on the infrapyloric region containing the infrapyloric artery (IPA) and lymph nodes.
Methods The anatomy of the IPA and its associated lymph nodes was clinically elucidated during 156 laparoscopic gastrectomies.
Results Most of the arteries originated from the anterior superior pancreatoduodenal artery (ASPDA, 64.2 %) or the root of the right gastroepiploic artery (RGEA, 23.1 %), but a small portion originated from the gastroduodenal artery (GDA, 12.7 %). The average lengths from the pyloric ring to the IPA proximal branch were 21.8 mm from the ASPDA, 20.6 mm from the RGEA and 9.0 mm from the GDA, a significantly shorter length than the other 2 variations. On average, 2.5 out of 10.0 nodes existed along the IPA. One patient, whose tumor was located close to the pylorus, had a metastatic node in this section.
Conclusion The IPA most commonly originates from the ASPDA and is associated with a certain number of lymph nodes. Vascular distribution from the IPA depends on the anatomic variation.

Keywords Infrapyloric artery · Station no.6 · Lymphadenectomy · Laparoscopic surgery · Gastric cancer

Introduction

The lymph nodes (LNs) lying in the infrapyloric area, categorized as the no. 6 by the Japanese Gastric Cancer Association (JGCA) [1], is considered an important confluence of lymphatic channels that drain the distal two-thirds of the stomach [2–4]. Several studies have demonstrated that metastasis to the no. 6 nodes is very common; thereby making the dissection of this station an important surgical step [5, 6]. JGCA has defined the no. 6 station as the area along the proximal part of the right gastroepiploic artery (RGEA) and vein [1]. That may make sense because most of lymphatic channels are accompanied by feeding vasculatures. However, blood flow to the pyloric antrum is predominantly supplied by the infrapyloric artery (IPA) [7, 8]. If the IPA is independent of the RGEA and is associated with regional LNs, anatomical knowledge of this artery will be required not only for the pylorus preserving procedures but also for the reasonable dissection of the infrapyloric region.

Despite previous angiography and cadaver autopsy studies, the anatomy of the IPA is poorly understood because it is too small for precise examination [9–13]. Recent advances in laparoscopic techniques, however, have provided surgeons with magnified and highly defined images [14–17]. In the present study, we elucidated the anatomy of the IPA by precisely identifying and dividing this artery during no. 6 lymphadenectomy. Also, the distribution of IPA tributaries to the pylorus and the number and metastatic status of LNs situated along the artery were investigated using surgical specimens.

S. Haruta and H. Shinohara contributed equally to this work.

S. Haruta · H. Shinohara (✉) · M. Ueno · H. Udagawa
Department of Gastroenterological Surgery, Toranomon Hospital, 2-2-2 Toranomon, Minato-ku, Tokyo 105-8470, Japan
e-mail: shinohara@toranomon.gr.jp

S. Haruta · I. Uyama
Department of Surgery, Fujita Health University, Aichi, Japan

Y. Sakai
Department of Surgery, Kyoto University Graduate School of Medicine, Kyoto, Japan

Published online: 17 September 2014

Methods

Patients

This study included 156 patients who underwent laparoscopic gastrectomy for early gastric cancer, clinically estimated to be T1 in depth. The study was conducted between December 2011 and April 2014 at Toranomon Hospital in Tokyo, Japan. Total gastrectomies were performed in 29 patients and distal gastrectomies were performed in 127 patients. None of the patients underwent a pylorus-preserving gastrectomy (PPG); therefore, standard no. 6 lymphadenectomies were performed in all cases.

Identification and division of IPA during no. 6 lymphadenectomies

The surgical setting of our laparoscopic gastrectomies and our procedure for the no. 6 LN dissection has been described previously [2]. After division of the greater omentum, the transverse smesocolon was taken down to identify the confluence of the right gastroepiploic vein (RGEV) and the anterior superior pancreatoduodenal vein (ASPDV). Subsequently, the RGEV and the infrapyloric vein (IPV) were ligated with clips and the adipose tissue, with its included LNs, was carefully dissected from the anterior surface of the head of the pancreas.

Next, we detached the pancreatic parenchyma from the posterior wall of the duodenal bulb to expose the gastroduodenal artery (GDA). The RGEA root was isolated by dissecting away the surrounding adipose tissue and nerve fibers. At this point, we were usually able to decipher whether the IPA was branched from the distal side (ASPDA) or proximal side (GDA) of the RGEA, except in cases when the IPA branched from the caudal part of the RGEA. The RGEA was ligated with double clips at its root and then the IPA was subsequently ligated. Finally, the inferior wall of the duodenal bulb was skeletonized, and the no. 6 nodal region was removed *en bloc* with the gastric specimen.

Investigation of IPA distribution to the pyloric antrum

Following resection, the surgical specimen was submitted for investigation to determine the morphometric anatomy of blood vessels. The distance from the pyloric ring to the first branch off of the RGEA that supplies the greater curvature was measured. Additionally, vascular distribution from the IPA was examined by measuring the length from the pyloric ring to the first proximal branch point along the IPA.

Examination of no. 6 lymph nodes

The soft tissue, including the no. 6 nodes, was then divided into three sections, according to previously described criteria [2]. In short; section 6a is adjacent to the RGEA from its first gastric branch to its root, section 6v is adjacent to the RGEV, between the root of the RGEA and the confluence of the ASPDV, and section 6i is located adjacent to the IPA (Fig. 1). The section 6i was discriminated from the section 6a along the avascular area between the proximal branch of the IPA and the RGEA. LNs from each section were then harvested and prepared for histological examination.

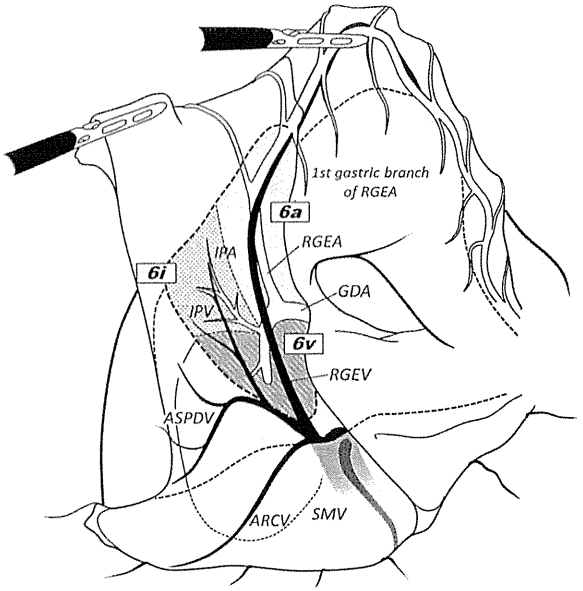

Fig. 1 The representative vascular anatomy of the infrapyloric lymph node station no. 6 that has been divided into three sections. These sections were divided along the proximal part of the right gastroepiploic vein (RGEV, 6v), the right gastroepiploic artery (RGEA, 6a), and the infrapyloric artery (IPA, 6i). *GDA* gastroduodenal artery, *ASPDV* anterior superior pancreatoduodenal vein, *IPV* infrapyloric vein, *SMV* superior mesenteric vein, *ARCV* accessory right colic vein, *GCT* gastrocolic trunk. This figure was quoted from Ref. [2] with some modifications under the permission of the authors

Statistics

Statistical analysis was performed using the unpaired Student's *t* test or the Chi square test. A *P*-value of less than 0.05 was regarded as statistically significant. All values henceforth are expressed in the following manner: mean (standard deviation).

Results

Origin of the IPA

The IPA was located and ligated intraoperatively in 115 cases and detected postoperatively in soft tissue specimens

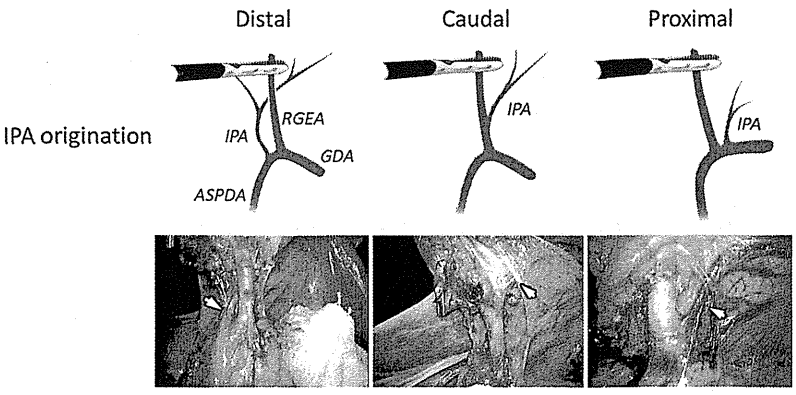

N	86 (64.2%)	31 (23.1%)	17 (12.7%)
IPA length	21.8 (8.4)‡	20.6 (7.6)‡	9.0 (3.2)
RGEA distance	47.8 (8.5)†	43.3 (8.6)†	36.2 (12.2)

Fig. 2 The origin of the infrapyloric artery (IPA) has been classified into three types: distal type, in which the IPA originates from the anterior superior pancreatoduodenal artery (ASPDA), caudal type, in which the IPA originates from the right gastroepiploic artery (RGEA), and proximal type, in which the IPA originates from the gastroduodenal artery (GDA). The *arrows* in the pictures indicate the origin of the IPA. *IPA length* represents the length from the pyloric ring to the proximal branch of the IPA (mm); *RGEA distance* represents the distance from the pyloric ring to the first gastric branch of the RGEA (mm). Values in parentheses represent the relative standard deviations. $^{\ddagger}P < 0.01$, $^{\dagger}P < 0.05$ compared with Proximal type

in the remaining 41 cases. In the latter set of cases, the origin of the IPA was identified in 19 out of 41 specimens. Therefore, a total of 134 samples were eligible for this study. The arteries from which the IPA originated were classified into three types: distal type (with the IPA originating from the ASPDA), proximal type (from the GDA), and caudal type (from the RGEA) (Fig. 2). Eighty-six cases (64.2 %) were categorized as distal type, 17 cases (12.7 %) were categorized as proximal type, and 31 cases (23.1 %) including all of the 19 cases in which the origin IPA was detected in the specimens after surgery were categorized as caudal type (Fig. 2). The branching points in 28 out of 86 distal type cases and 7 out of 17 proximal type cases were, however, very close to the root of the RGEA.

Vascular distribution from the IPA

We examined the distribution of the IPA tributaries in the surgical specimens. Results and representative pictures of distal and caudal types are summarized in Fig. 2 and shown in Fig. 3, respectively. The lengths from the pyloric ring to the proximal branch of the IPA were 21.8 mm (8.4) and 20.6 mm (7.6) in distal and caudal types, respectively. These were significantly longer than the average value of the proximal type, which was 9.0 mm (3.2) in length. The distances from the pyloric ring to the first gastric branch of the RGEA, which corresponds to the width of no. 6 area, were 47.8 mm (8.5) for the distal type and 43.3 mm (8.6) for caudal type. Similarly, these were significantly longer than the value of the proximal type, which was 36.2 mm (12.2) in width.

Lymph nodes in the infrapyloric area

Finally, we examined how many LNs existed along the IPA. On average, 5.0 (3.2), 2.5 (2.0) and 2.5 (2.1) LNs were harvested from the sections 6a, 6v and 6i, respectively. Metastases to no. 6 were found in 5 out of 156 patients. Four patients had a metastatic LN in section 6a and 1 patient had three metastatic nodes in section 6v. One patient, who had a T1 tumor of the antrum, 2 cm proximal to the pylorus, had a metastatic node in section 6i.

Discussion

Among the regional LNs of the stomach, the no. 6 infrapyloric nodes lie in an anatomically important area. The JGCA has defined the "afferent section" as the area along the first branch and the proximal section of the RGEA; the "efferent section" is defined as the area from the border of the afferent section to the confluence of the RGEV and the ASPDV [1]. Blood flow from the pyloric antrum, however, is predominantly supplied by its own artery, the IPA [9]. Thus, we focused on the anatomy of this artery and its associated LNs.

The IPA, a small artery whose diameter is approximately 1.2 mm [9], was initially described in 1904 as

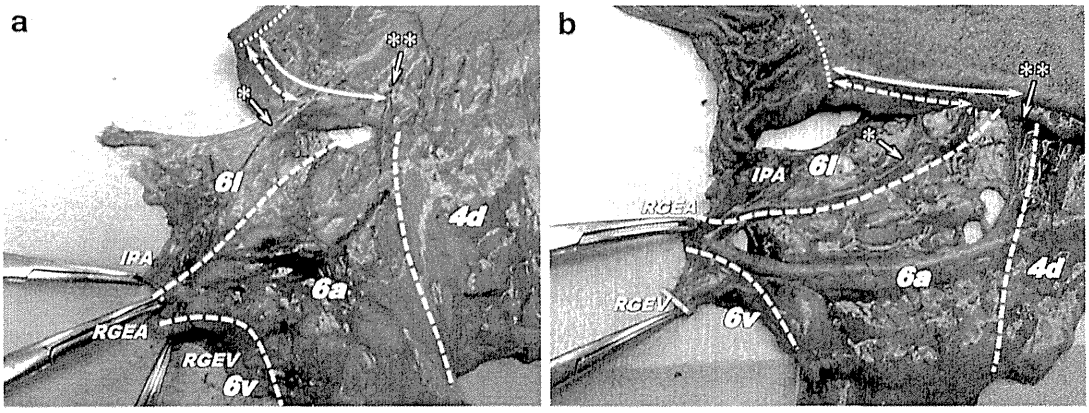

Fig. 3 Representative distal-type **a** and caudal-type **b** surgical specimens, demonstrating the infrapyloric lymph station no. 6 vasculature divided into three sections. *Dotted lines* indicate the pyloric ring, *dashed arrows* indicate the length from the pyloric ring to the proximal branch of the infrapyloric artery (IPA, *asterisk*), and *solid arrows* indicate the distance from the pyloric ring to the first gastric branch of the right gastroepiploic artery (RGEA, *double asterisk*). *RGEV* right gastroepiploic vein

"Ciuffo pilorico inferior" by Rossi et al. [10], and identified as the "pyloric branch" in 1982 by Kuroda et al. [11]. The term "infrapyloric artery" was first cited in 1988, referring to the IPA originating from the RGEA [12]. Studies evaluating the origin of the IPA, however, vary throughout the literature. Sawai et al. [13] reported that the IPA originates from the GDA in 64 %, from the ASPDA in 21 %, and from the RGEA in only 12 % of gastric cancer patients, determined via angiography. In contrast, a recent study by Takamuro et al. [9] using 214 cadavers confirmed that nearly 50 % of IPAs originate from the ASPDA or from the wedged position, between the ASPDA and RGEA. In the present study, which included 134 early gastric cancer surgeries, we have carefully explored the origins of the IPA around the root of the RGEA with precise laparoscopic images. Our results demonstrate that most of the IPAs originated from the previously defined distal or caudal site; however only 12.7 % originated proximal to the root of the RGEA. These data support the findings obtained from the cadaver study by Takamuro et al. [9]. Discrepancies from previous reports may be due to the difficulty in identifying these arteries because of their small diameters.

The average number of LNs harvested from section 6i (along the IPA) was 2.5. Although we did not detect lymphatic vessels, our data suggest the existence of afferent lymphatic fluid that flows alongside the IPA from the pyloric antrum to the root of the RGEA. In the present study, one patient whose tumor was located in the antrum fed by the IPA had metastases to this section. Conversely, it may be possible to exclude the section 6i dissection in patients undergoing a PPG with an indication directly based on tumor location and depth of invasion.

In conclusion, the IPA predominantly feeds the pyloric antrum, usually originates from the ASPDA and is accompanied by a certain number of LNs. Consideration of the findings of this study will provide for safer, more oncologically feasible lymph node dissection of the infrapyloric region in gastric cancer surgery.

Acknowledgments We thank Dr. Kyle J. Litow for English proofreading.

References

1. Japanese Gastric Cancer Association. Japanese classification of gastric carcinoma: 3rd English edition. Gastric Cancer. 2011;14:101–12.
2. Shinohara H, Kurahashi Y, Kanaya S, Haruta S, Ueno M, Udagawa H, et al. Topographic anatomy and laparoscopic technique for dissection of no. 6 infrapyloric lymph nodes in gastric surgery. Gastric Cancer. 2013;16(4):615–20.
3. Pólya E, von Navratil D. Untersuchung űber die Lymphbahnen des Wurmfortsatzes und des Magens. Zeitschr fűr klin Chir. 1903;69:421–56.
4. Pólya E. Zur Stumpfversorgung nach Magenresektion. Zentrbl fűr Chir. 1911;38:892–4.
5. Sasako M, McCulloch P, Kinoshita T, Maruyama K. New method to evaluate the therapeutic value of lymph node dissection for gastric cancer. Br J Surg. 1995;82:346–51.
6. Maruyama K, Gunvēn P, Okabayashi K, Sasako M, Kinoshita T. Lymph node metastases of gastric cancer. General pattern in General pattern in 1931 patients. Ann Surg. 1931;1989(210):596–602.
7. Liberski SM, Koch KL, Atnip RG, Stern RM. Ischemic gastroparesis: resolution after revascularization. Gastroenterology. 1990;99:252–7.
8. Wilkie D. Blood supply of the duodenum. Surg Gynecol Obstet. 1911;3:399–405.
9. Takamuro T, Murakami G, Hirata K. Arterial supply of the first, third and fourth portion of the duodenum: an anatomical study with special reference to the minimal invasive

pancreaticoduodenectomy (in Japanese). Jpn J Gastroenterol Surg. 1998;31:825–35.
10. Rossi G, Cova E. Studio morfolgico delle arterie dello stomaco. Arch Ital Anat Embriol. 1904;3:485.
11. Kuroda C, Nakamura H, Sato T, Yoshioka H, Tokunaga K, Hori S, et al. Normal anatomy of the pyrolic branch and its diagnostic significance in angiography. Acta Radiol Diagn. 1982;23:479–84.
12. Vandamme J, Bonte J. The blood supply of the stomach. Acta Anat. 1988;131:89–96.
13. Sawai K, Takahashi T, Fujioka T, Minato H, Tanigushi H, Yamagushi T. Pylorus-preserving gastrectomy with radical lymph node dissection based on anatomical variations of the infrapyloric artery. Am J Surg. 1995;170:285–8.
14. Uyama I, Sugioka A, Matsui H, Fujita J, Komori Y, Hasumi A. Laparoscopic D2 lymph node dissection for advanced gastric cancer located in the middle or lower third portion of the stomach. Gastric Cancer. 2000;3:50–5.
15. Kanaya S, Haruta S, Kawamura Y, Yoshimura F, Inaba K, Hiramatsu Y, et al. Laparoscopy distinctive technique for suprapancreatic lymph node dissection: medial approach for laparoscopic gastric cancer surgery. Surg Endosc. 2011;25:3928–9.
16. Obama K, Okabe H, Hosogi H, Tanaka E, Itami A, Sakai Y. Feasibility of laparoscopic gastrectomy with radical lymph node dissection for gastric cancer: from a viewpoint of pancreas-related complications. Surgery. 2011;149:15–21.
17. Noshiro H, Nagai E, Shimizu S, Uchiyama A, Tanaka M. Laparoscopically assisted distal gastrectomy with standard radical lymph node dissection for gastric cancer. Surg Endosc. 2005;19:1592–6.

Ann Surg Oncol
DOI 10.1245/s10434-014-3670-1

Annals of
SURGICAL ONCOLOGY
OFFICIAL JOURNAL OF THE SOCIETY OF SURGICAL ONCOLOGY

ORIGINAL ARTICLE – GASTROINTESTINAL ONCOLOGY

Low Creatinine Clearance is a Risk Factor for D2 Gastrectomy after Neoadjuvant Chemotherapy

Tsutomu Hayashi, MD[1], Toru Aoyama, MD[1], Kazuaki Tanabe, MD[2], Kazuhiro Nishikawa, MD[3], Yuichi Ito, MD[4], Takashi Ogata, MD[1], Haruhiko Cho, MD[1], Satoshi Morita, PhD[5], Yumi Miyashita[6], Akira Tsuburaya, MD[7], Junichi Sakamoto, MD[8], and Takaki Yoshikawa, MD[1]

[1]Department of Gastrointestinal Surgery, Kanagawa Cancer Center, Asahi-Ku, Yokohama, Japan; [2]Department of Gastrointestinal Surgery, Hiroshima University, Hiroshima, Japan; [3]Department of Surgery, Osaka General Medical Center, Osaka, Japan; [4]Department of Gastroenterological Surgery, Aichi Cancer Center, Nagoya, Japan; [5]Department of Biostatistics and Epidemiology, Yokohama City University Medical Center, Yokohama, Japan; [6]Data center, Nonprofit Organization ECRIN, Okazaki, Japan; [7]Clinical Research Center, Shonan Kamakura General Hospital, Kamakura, Japan; [8]Tokai Central Hospital, Kakamigahara, Japan

ABSTRACT

Background. The feasibility and safety of D2 surgery following neoadjuvant chemotherapy (NAC) has not been fully evaluated in patients with gastric cancer. Moreover, risk factor for surgical complications after D2 gastrectomy following NAC is also unknown. The purpose of the present study was to identify risk factors of postoperative complications after D2 surgery following NAC.

Methods. This study was conducted as an exploratory analysis of a prospective, randomized Phase II trial of NAC. The surgical complications were assessed and classified according to the Clavien–Dindo classification. A uni- and multivariate logistic regression analyses were performed to identify risk factors for morbidity.

Results. Among 83 patients who were registered to the Phase II trial, 69 patients received the NAC and D2 gastrectomy. Postoperative complications were identified in 18 patients and the overall morbidity rate was 26.1 %. The results of univariate and multivariate analyses of various factors for overall operative morbidity, creatinine clearance (CCr) $\leq$ 60 ml/min ($P = 0.016$) was identified as sole significant independent risk factor for overall morbidity. Occurrence of pancreatic fistula was significantly higher in the patients with a low CCr than in those with a high CCr.

Conclusions. Low CCr was a significant risk factor for surgical complications in D2 gastrectomy after NAC. Careful attention is required for these patients.

Gastric cancer is the second most frequent cancer-related cause of death after lung cancer.[1] Complete resection is essential for the cure of gastric cancer. After the long debate, D2 gastrectomy has been established as a standard surgical procedure not only in Japan and Korea, but also in Europe and United States.[2–5]

Recently, several large phase III studies demonstrated that multimodality treatment, including surgery, significantly improved the survival of locally advanced disease compared with surgery alone; postoperative adjuvant chemotherapy with S-1 in Japan, postoperative adjuvant chemotherapy with capecitabine plus oxaliplatin in Korea, and pre- and postoperative chemotherapy in United Kingdom.[6–8] Neoadjuvant chemotherapy is a promising treatment for gastric cancer when considering intensive chemotherapy with relatively toxic regimen.[9] Neoadjuvant chemotherapy is tested in several phase III trials in the eastern Asia where D2 and adjuvant chemotherapy is a standard treatment.[10,11] Although D2 gastrectomy is a feasible and safe procedure as a primary treatment when performed by experienced surgeons, the feasibility and safety of D2 surgery following neoadjuvant chemotherapy has not been fully evaluated. Two positive phase III trials performed in United Kingdom and France demonstrated

Tsutomu Hayashi and Toru Aoyama have contributed equally to this work.

First Received: 12 July 2013

T. Yoshikawa, MD
e-mail: yoshikawat@kcch.jp

Published online: 09 April 2014

that the surgical morbidity and mortality were almost similar between surgery alone and surgery following the neoadjuvant chemotherapy; however, the surgical procedures were less than D2 in most cases in the UK study and were not accurately described in the French study.[8,12] Only one European phase III study has compared D2 alone and D2 following the neoadjuvant chemotherapy. In that study, the overall morbidity was higher and injury of major blood vessels was more frequent in the neoadjuvant group than in the surgery alone group.[13]

Generally, chemotherapy acts for tumor tissue and induces variety changes of both tumor and stroma including necrosis, inflammation, and fibrosis, which makes D2 surgery difficult.[14] Although experienced surgeons may complete D2 after neoadjuvant chemotherapy safely as reported in several Japanese phase II studies of single arm, surgical complication is unavoidable.[15–18] Accidental in jury of major blood vessels during surgery may cause lethal complication. If risk factor for complications is clarified, it becomes possible to determine appropriate indication and surgical procedure considering the balance between the risk and the benefit.

Previously, only Fujitani et al. reported that age greater than 60 years and high body mass index were significant risk factors for overall complications in 71 patients who received gastrectomy following induction chemotherapy and preoperative chemoradiotherapy in the retrospective analysis of M.D. Anderson Cancer Center.[19] However, their report was based on a retrospectively collected data in which most patients received induction chemoradiotherapy. Complication was not determined following Clavien-Dindo classification. Moreover, surgical procedure had not been strictly limited to D2.

The purpose of the present study is to identify risk factors of postoperative complications after D2 surgery following neoadjuvant chemotherapy. This study was conducted as an exploratory analysis of a prospective, randomized, Phase II trial of neoadjuvant chemotherapy.

PATIENTS AND METHODS

The patients who received neoadjuvant chemotherapy and D2 gastrectomy as a protocol treatment in the phase II trial were examined in this study. The details of this trial were described in the previous report.[20,21] Briefly, key eligibility included clinical T2-3/N+ or clinical T4aN0 in case of scirrhous or junction tumors, clinical T2-3 with nodal metastasis to the major branched artery, clinical T4aN+, clinical T4b, para-aortic nodal metastases, or resectable minimal peritoneal metastases confirmed by laparoscopy. Staging laparoscopy was mandatory to diagnose peritoneal metastasis. Eligible patients were randomized to two courses of S-1 plus cisplatin, four courses of S-1 plus cisplatin, two courses of Paclitaxel plus cisplatin, or four courses of Paclitaxel plus cisplatin. The sample size was calculated to be 60–80 in a total considering a statistical power of approximately 0.8.

Neoadjuvant Chemotherapy

In S-1 plus cisplatin regimen, S-1 80 mg/m^2 was given orally twice daily for the first 3 weeks of a 4-week cycle and cisplatin was given as an intravenous infusion of 60 mg/m^2 on day 8 of each cycle as described previously.[20,21] In Paclitaxel plus cisplatin regimen, Paclitaxel 60 mg/m^2 and cisplatin 25 mg/m^2 were administered on days 1, 8, and 15 as 1 course, repeated every 4 weeks.[20,21] Neoadjuvant chemotherapy was discontinued if there was documented disease progression, unacceptable toxicity, or withdrawal of consent.

Surgery

During 2–6 weeks after completion of neoadjuvant chemotherapy or when the tumors progressed during the treatment, patients proceeded to surgery. R0 resection was aimed by gastrectomy with standard D2 lymphadenectomy.[2] Para-aortic nodal dissection or combined resection of small part of the peritoneum or adjacent organs are permitted for the curative intent but more invasive surgery, such as pancreaticoduodenectomy or Appleby's surgery are not. When macroscopically curative surgery was achieved, protocol treatment was terminated.

Evaluation

Clinical diagnosis of T and N was determined by thin-slice CT with 5- to 7-mm thickness or multidetector low CT following Habermann's method.[22] T1 tumors were defined as those that could not be found on the images or those with focal thickening of the inner layer with a visible outer layer of the gastric wall and a clear fat plane around the tumor. T2-3 tumors were defined as those with focal or diffuse thickening of the gastric wall with transmural involvement and a smooth outer border of the wall or only a few small linear strands of soft tissue extending into the fat plane involving less than one-third of the tumor extent. T4a tumors were defined as transmural tumors with obvious blurring of at least one-third of the tumor extent or wide reticular strands surrounding the outer border of the tumor. T4b tumors were defined as those with obliteration of the fat plane between the gastric tumor and the adjacent organ or invasion of an adjacent organ. Regional lymph nodes were considered to be involved by metastases if they were larger than 8 mm in the short-axis diameter. Progression of tumors was evaluated by the 14th edition of the Japanese Gastric Cancer Classification.[2] Clinical response of the lymph node was evaluated by

version 1.0 of the Response Evaluation Criteria for Solid Tumors.[23] The surgical complications were assessed and classified according to the Clavien–Dindo classification.[24] The incidence of reoperation and the length of hospital stay also were recorded. Operative mortality was defined as postoperative death from any cause within 30 days after surgery or during the same hospital stay.

Statistical Analysis

A uni- and multivariate logistic regression analyses was performed to identify risk factors for morbidity. Comparisons between the two groups were analyzed by chi-square test. In the multivariate analysis, we fitted linear regression models. To select a model, we used backward elimination. All statistical tests were two-sided, and significance was set at $P < 0.05$.The SPSS software package (v11.0 J Win, SPSS, Chicago, IL) was used for all statistical analyses.

Ethical Review

The COMPASS phase II trial had been approved in all institutions and confirmed to all patients who registered to this trial. This exploratory analysis was attached to the COMPASS phase II trial.

RESULTS

Patient's Characteristics

Between October 2009 and July 2011, a total of 83 patients were registered to the COMPASS trial. Among them, 69 patients received the neoadjuvant chemotherapy and D2 gastrectomy. On the other hands, 14 patients did not receive gastrectomy because curative D2 surgery was not possible. Six patients did not receive surgery based on the CT findings, two received bypass surgery because of the stenosis of the primary lesion, and six underwent palliative D1 surgery due to bleeding or stenosis. Characteristics of 69 patients before neoadjuvant chemotherapy are shown in Table 1. The operative details are shown in Table 2. The background factors and operative procedures were well balanced between the two regimens.

Operative Morbidity and Mortality

Postoperative complications were found in 18 among 69 patients (26.1 %). No surgical mortality was observed. Details of complications are shown in Table 3. Pancreatic fistula was found in 13 % in all grades and in 1.4 % in grade 3 or more, anastomotic leakage was 4.3 % in all grades and in 2.9 % in grade 3 or more, and abdominal abscess was 4.3 % in all grades and in 1.4 % in grade 3 or more. No patient required reoperation. No mortality was observed.

Risk Factors for Operative Morbidity

Risk factors for surgical morbidity were analyzed by uni- and multivariate analyses using clinical factors determined before the enrollment of the study. The results are summarized in Table 4. Among these, creatinine clearance (CCr) $\leq$ 60 ml/min ($P = 0.016$) was identified as sole significant independent risk factor for overall morbidity. Median value of CCr (range) was 54 ml/min (42–60 ml/min) in patients with creatine clearance $\leq$60 ml/min and 78 ml/min (61–143 ml/min) in patients with creatine clearance >60 ml/min. Table 5 shows the details of the complications after D2 gastrectomy between the two groups. Occurrence of pancreatic fistula was significantly different between the two groups. Pleural effusion was tended to be higher in patients with creatine clearance $\leq$60 ml/min compared with patients with creatine clearance >60 ml/min.

DISCUSSION

This is the first report to evaluate the risk factors for morbidity of D2 gastrectomy after neoadjuvant chemotherapy (NAC) in patients with gastric cancer. The present study demonstrated that creatinine clearance (CCr) was the only independent risk factor for surgical complications. Therefore, careful attention is required in patients with low CCr when surgeons consider D2 gastrectomy after NAC.

In this study, creatinine clearance (CCr) was the only independent risk factor for surgical complications in the patients who received D2 gastrectomy after NAC. Generally, impaired renal function had the decreased immunity, decreased ability of wound healing, prolonged fluid retention, and anemia.[25] Prolonged fluid retention may cause peripheral edema, ascites, and pleural effusion. In the present study, pleural effusion was tended to be high in patients with low CCr. Moreover, the patients with low CCr had more pancreatic fistula than those with high CCr. However, previous reports demonstrated that renal function was not selected as risk factor for primary surgery.[26,27] Renal function is related with clearance of anticancer drug, such as Cisplatin (CDDP).[28] High concentration of CDDP in the patients with low CCr may cause more tissue damage than those with high CCr, which may be related to complications.[14] Moreover, median value of CCr in patients with low CCr was 54 ml/min, which suggested that their renal function was not severely disturbed. Exact mechanisms for CCr as a risk factor should be clarified in the future.

TABLE 1 Patient's characteristics

	S-1 + Cisplatin	Paclitaxel + Cisplatin	Total
Patients number	34	35	69
Male/female	23/11	26/9	49/20
Age (yr), median (range)	66 (32–79)	66 (44–77)	66 (32–77)
Performance status 0/1	34/0	34/1	68/1
BMI (kg/m^2), median (range)	21.1 (16.9–25.2)	21 (15.9–27)	21 (15.9–27)
Creatinine clearance (ml/min), median (range)	74.8 (42–120.4)	75.3 (47–143)	75 (42–143)
Clinical T factor 3/4a/4b	2/29/3	4/30/1	6/59/4
Clinical N factor 0/1/2	5/24/5	7/26/2	12/50/7
Metastasis status			
Negative	32	31	63
Cytology positive	2	4	6
Peritoneal metastasis	0	0	0
Esophagus invasion			
Negative	24	23	47
Positive	10	12	22
Macroscopic tumor type			
0	0	1	1
1	1	4	5
2	9	10	19
3	16	15	31
4	3	3	6
5	5	2	7
Pathologic tumor type			
Differentiated	14	15	29
Undifferentiated	20	20	40
Actual course of neoadjuvant chemotherapy			
1	2	1	3
2	21	16	37
3	1	2	3
4	10	16	26
Clinical response			
Complete response	1	0	1
Partial response	14	10	24
Stable disease	18	24	42
Progression disease	1	1	2

In the present study, age was a marginally significant risk factor in the univariate analysis but not in the multivariate analysis. Elderly patients often have comorbidities and age-related physiological problems, such as organ dysfunction. Fujitani et al. also demonstrated that age was one of risk factor for complications in patients who received gastrectomy following induction chemoradiotherapy.[19] Several reports showed that age was a risk factor for surgical complication for primary gastric cancer surgery.[26,27] Dutch phase III trial comparing D1 and D2 showed that age older than 65 years was a significant risk factor for hospital death and overall complications.[26] Kohn reported that many organ function decreases linearly after 30 years old.[29] Actually, the elderly patients had higher risk with 32 % than that of the nonelderly with 10.5 %. On the other hand, among the elderly, patients with high CCr had 25 % of morbidity, whereas those with low CCr had very high risk with 83.3 %. Thus, surgical risk could be well separated by combining CCr. CCr was significantly correlated with age ($r = -0.468$ and $P = 0.000$ by Pearson's correlation coefficient) in this cohort. CCr was significantly related with age in this cohort ($r = -0.468$,

TABLE 2 Operative details

	S-1 + Cisplatin	Paclitaxel + Cisplatin	Total
Gastrectomy			
Total	25	27	52
Distal	9	8	17
Esophagogastrectomy, yes/no	10/24	12/23	22/47
Splenectomy, yes/no	16/18	22/13	38/31
Pancreatectomy, yes/no	0/34	2/33	2/67
Bulsectomy, yes/no	3/31	7/28	10/59
Mediastinal lymphadenectomy			
None	34	34	68
Transhiatal	0	1	1
Blood loss (ml), median (range)	430 (60–1300)	440 (70–1990)	440 (60–1990)
Operation time (min), median (range)	242 (155–422)	262 (172–381)	254 (155–422)

TABLE 3 Details of complications

	Grade 1	Grade 2	Grade 3a/3b	Grade 4a/4b	Grade 5
Pancreatic fistula	4	4	1/0	0	0
Abdominal abscess	0	2	1/0	0	0
Anastomotic leakage	0	1	2/0	0	0
Pneumonia	1	0	0	0	0
Postoperative bleeding	1	2	1/0	0	0
Wound abscess	0	1	0	0	0
Anastomotic stenosis	0	1	0	0	0
Pleural effusion	2	0	0	0	0

$P = 0.000$ by Pearson's correlation coefficient). Morbidity rate was related with CCr in the elderly patients (11/44 in the patients with high CCr and 5/6 in those with low CCr), but the relationship was uncertain in the nonelderly patients (2/17 in the patients with high CCr and 0/2 in those with low CCr) because of small numbers. Generally, CCr decreases in the elderly patients. A value of CCr as a risk factor may be in the elderly patients.

In the primary D2 surgery, splenectomy and body mass index (BMI) were reportedly identified as the most significant independent risk factors.[26,30] However, splenectomy was not a risk factor both in uni- and multivariate analyses in the present study. This may be due to the difference of tumor progression and the effect of neoadjuvant chemotherapy. In the present study, most patients had clinical nodal metastases. Nodal dissection itself may become difficult due to fibrotic changes after neoadjuvant chemotherapy, which may increase the minimal risk due to spleen-preserving surgery up to the high risk observed in splenectomy. More, BMI was not an independent risk factor in this study, in contrast to JCOG9501 trial in which BMI >25 kg/m^2 was a significant risk factor for major surgical complications.[31] This discrepancy may be attributed to lower incidence of BMI > 25 kg/m^2. The proportion of patients BMI > 25 kg/m^2 was 7.2 % (5/69) in the present series as opposed to 14.7 % (77/523) in the JCOG9501 trial.

The present study has some limitations. First, sample size was relatively small, although this study is an exploratory analysis of prospective, multicenter, randomized phase II study. Second, our results would not be applicable for the different cohort, which has different tumor stage. Different risk factor may be selected if other cohort has relatively early disease for which prophylactic nodal dissection is enough. Third, the present study used the clinical data before the study entry other than the clinical response. We considered that surgical difficulties depended on the tumor progression before the chemotherapy. On the other hand, CCr or body mass index may change after chemotherapy. Although the CCr just before surgery was not collected in this study, CCr would be not changed or worsened in most cases. Body weight may decrease in some cases after chemotherapy. Thus, our results would underestimate the impact of CCr as risk factor but not overestimate. Forth, optimal cutoff values were unknown. In this study, we used the 60 ml/min as the cutoff value of CCr and 60 years as the cutoff value of age. Distribution, median, and average of the CCr of all patients were 41.0–143.0 ml/min, 73.15 ml/min, and 78.3 ± 19.1 ml/min. CCr of 60 ml/min was lower limit to guarantee the "unimpaired renal function" and was selected as one of the stratification factors in this trial. Therefore, we used the 60 ml/min as the cutoff value of CCr. Median age

TABLE 4 Univariate and multivariate analyses of risk factors for complications

Factors	No	No. of complications	Univariate analysis		Multivariate analysis	
			Relative risk	*P*	Relative risk	*P*
Age (yr)				0.086		
<60	19	2	1.000			
≥60	50	16	4.000 (0.823–19.44)			
Gender				0.19		
Female	20	3	1.000			
Male	49	15	2.499 (0.635–9.828)			
Body mass index				0.496		
<25	64	16	1.000			
≥25	5	2	2.000 (0.306–13.061)			
Type of gastrectomy				0.782		
Distal gastrectomy	17	4	1.000			
Total gastrectomy	52	14	1.197 (0.334–4.295)			
Splenectomy and/or pancreatomy				0.615		
Yes	38	9	1.000			
No	31	9	1.318 (0.449–3.871)			
Bulsectomy				0.761		
No	59	15	1.000			
Yes	10	3	1.257 (0.288–5.49)			
Clinical response				0.785		
SD-PD	44	11	1.000			
CR-PR	25	7	1.167 (0.385–3.5133)			
Clinical tumor invasion				0.674		
T4a	63	16	1.000			
T3	6	2	1.469 (0.245–8.794)			
Clinical lymph node metastasis				0.155		
N (−)	12	1	1.000			
N (+)	57	17	4.675 (0.559–39.113)			
Clinical esophagus invasion				0.562		
No	47	12	1.000			
Yes	22	6	1.094 (0.348–3.436)			
Clinical stage				0.587		
IV	6	1	1.000			
II or III	63	17	1.848 (0.201–16.974)			
Chemotherapy regimen				0.246		
Paclitaxel + Cisplatin	35	7	1.000			
TS-1 + Cisplatin	34	11	1.913 (0.639–5.727)			
Chemotherapy course				0.754		
3–4	29	7	1.000			
1–2	40	11	1.192 (0.398–3.573)			
Creatinine clearance (ml/min)				0.022		0.016
>60	61	13	1.000		1.000	
≤60	8	5	6.154 (1.297–29.197)		8.666 (1.487–50.509)	

of all the patients was 66 (range 32–79) years in this trial. Previously, Fujitani et al. demonstrated that age was one of risk factor for complications in patients who received gastrectomy following induction chemoradiotherapy.[19] In that report, they set the cutoff value as 60 years. Therefore, we set the cutoff value as 60 years in this study. Appropriate cutoff value should be determined in the other validation studies.

TABLE 5 Operative morbidity between CCr $\leq$ 60 ml/min and CCr > 60 ml/min

	CCr $\leq$ 60 ml/min (n = 8)		CCr > 60 ml/min (n = 61)		P
	No. of patients	(%)	No. of patients	(%)	
Pancreatic fistula	4	50	5	8.2	0.004
Abdominal abscess	1	12.5	2	3.3	0.215
Anastomotic leakage	0	0	3	4.9	0.814
Pneumonia	0	0	1	1.6	0.715
Postoperative bleeding	0	0	4	6.6	0.906
Wound abscess	0	0	1	1.6	0.715
Anastomotic stenosis	0	0	1	1.6	0.715
Pleural effusion	1	12.5	1	1.6	0.085

In summary, low CCr was a significant risk factor for surgical complications in D2 gastrectomy after NAC. Careful attention is required for these patients when surgeons consider D2 gastrectomy after NAC.

ACKNOWLEDGMENT The authors are grateful to Professor Morita of the Department of Biomedical Statistics and Bioinformatics, Graduate School of Medicine and Faculty of Medicine, Kyoto University, for his kind support for the statistical consideration and advice. This work is supported by Epidemiological & Clinical Research Information Network (ECRIN).

CONFLICT OF INTEREST None declared.

REFERENCES

1. Ohtsu A, Yoshida S, Saijo N. Disparities in gastric cancer chemotherapy between the East and West. *J Clin Oncol.* 2006;24: 2188–96.
2. Japanese Gastric Cancer Association. Japanese classification of gastric carcinoma: 3rd English edition. *Gastric Cancer.* 2011;14: 101–12.
3. Park JM, Kim YH. Current approaches to gastric cancer in Korea. *Gastrointest Cancer Res.* 2008;2:137–44.
4. Okines A, Verheij M, Allum W, Cunningham D, Cervantes A; ESMO Guidelines Working Group. Gastric cancer: ESMO clinical practice guidelines for diagnosis, treatment and followup. *Ann Oncol.* 2010;21(Suppl 5):v50–4.
5. NCCN. NCCN Clinical Practice Guidelines in Oncology. Gastric Cancer. Version 2.2011. 2011. http://www.nccn.org. Accessed 5 Dec 2011.
6. Sakuramoto S, Sasako M, Yamaguchi T, Kinoshita T, Fujii M, Nashimoto A, et al. Adjuvant chemotherapy for gastric cancer with S-1, an oral fluoropyrimidine. *N Engl J Med.* 2007;357:1810–20.
7. Bang YJ, Kim YW, Yang HK, Chung HC, Park YK, Lee KH, et al. Adjuvant capecitabine and oxaliplatin for gastric cancer after D2 gastrectomy (CLASSIC): a phase 3 open-label, randomized controlled trial. *Lancet.* 2012;28:315–21.
8. Cunningham D, Allum WH, Stenning SP, Thompson JN, Van de Velde CJ, Nicolson M, et al. Perioperative chemotherapy versus surgery alone for resectable gastroesophageal cancer. *N Engl J Med* 1993;355:11-20.
9. Yoshikawa T, Rino Y, Yukawa N, Oshima T, Tsuburaya A, Masuda M. Neoadjuvant chemotherapy for gastric cancer in japan: a standing position by comparing with adjuvant chemotherapy. *Surg Today.* 2013;44(1):11–21.
10. Docetaxel+Oxaliplatin+S-1 (DOS) Regimen as Neoadjuvant Chemotherapy in Advanced Gastric Cancer (PRODIGY). ClinicalTrials.gov Identifier: NCT01515748.
11. SOX Regimen as Neoadjuvant Chemotherapy for AJCC Stage II-III Gastric Cancer (RESONANCE). ClinicalTrials.gov Identifier: NCT01583361.
12. Ychou M, Boige V, Pignon JP, Conroy T, Bouche O, Lebreton G, et al. Perioperative chemotherapy compared with surgery alone for resectable gastroesophageal adenocarcinoma: an FNCLCC and FFCD multicenter phase III trial. *J Clin Oncol.* 2011;29: 1715–21.
13. Schuhmacher C, Gretschel S, Lordick F, Reichardt P, Hohenberger W, Eisenberger CF, et al. Neoadjuvant chemotherapy compared with surgery alone for locally advanced cancer of the stomach and cardia: European Organisation for Research and Treatment of Cancer randomized trial 40954. *J Clin Oncol.* 2010;28:5210–8.
14. Wang ZH, Zhang SZ, Zhang ZY, Zhang CP, Hu HS, Kirwan J, et al. The influence of intraarterial high-dose cisplatin with concomitant irradiation on arterial microanastomosis: an experimental study. *Am J Clin Oncol.* 2009;32:158–62.
15. Yoshikawa T, Sasako M, Yamamoto S, Sano T, Imamura H, Fujitani K, et al. Phase II study of neoadjuvant chemotherapy and extended surgery for locally advanced gastric cancer. *Br J Surg.* 2009;96:1015–22.
16. Iwasaki Y, Sasako M, Yamamoto S, Nakamura K, Sano T, Katai H, et al. Phase II study of preoperative chemotherapy with S-1 and cisplatin followed by gastrectomy for clinically resectable type 4 and large type 3 gastric cancers (JCOG0210). *J Surg Oncol.* 2013;107:741–5.
17. Kinoshita T, Sasako M, Sano T, Katai H, Furukawa H, Tsuburaya A, et al. Phase II trial of S-1 for neoadjuvant chemotherapy against scirrhous gastric cancer (JCOG 0002). *Gastric Cancer.* 2009;12:37–42.
18. Tsuburaya A, Nagata N, Cho H, Hirabayashi N, Kobayashi M, Kojima H, et al. Phase II trial of paclitaxel and cisplatin as neoadjuvant chemotherapy for locally advanced gastric cancer. *Cancer Chemother Pharmacol.* 2013;71:1309–14.
19. Fujitani K, Ajani JA, Crane CH, Feig BW, Pisters PW, Janjan N, et al. Impact of induction chemotherapy and preoperative chemoradiotherapy on operative morbidity and mortality in patients with locoregional adenocarcinoma of the stomach or gastroesophageal junction. *Ann Surg Oncol.* 2007;14:2010–7.
20. Yoshikawa T, Tsuburaya A, Morita S, Kodera Y, Ito S, Cho H, et al. A comparison of multimodality treatment: two or four courses of paclitaxel plus cisplatin or S-1 plus cisplatin followed by surgery for locally advanced gastric cancer, a randomized Phase II trial (COMPASS). *Jpn J Clin Oncol.* 2010;40:369–72.
21. Yoshikawa T, Tanabe K, Nishikawa K, Ito Y, Matsui T, Kimura Y, et al. Induction of a pathological complete response by four courses of neoadjuvant chemotherapy for gastric cancer: early results of the randomized phase II COMPASS Trial. *Ann Surg Oncol.* 2014;21:213–9.
22. Habermann CR, Weiss F, Riecken R, Honarpisheh H, Bohnacker S, Staedtler S, et al. Preoperative staging of gastric adenocarcinoma: comparison of helical CT and endoscopic US. *Radiology* 2004;230:465–70.

23. Therasse P, Arbuck SG, Eisenhauer EA, et al. New guidelines to evaluate the response to treatment in solid tumors (RECIST guidelines) *J Natl Cancer Inst.* 2000;92:205–16.
24. Clavien PA, Barkun J, de Oliveira ML, Vauthey JN, Dindo D, Schulick RD, et al. The Clavien-Dindo classification of surgical complications: five-year experience. *Ann Surg* 2009;250: 187–96.
25. Vaziri ND, Pahl MV, Crum A, Norris K. Effect of uremia on structure and function of immune system. *J Ren Nutr.* 2012;22: 149–56.
26. Sasako M. Risk factors for surgical treatment in the Dutch Gastric Cancer Trial. *Br J Surg.* 1997;84:1567–71.
27. Kodera Y, Sasako M, Yamamoto S, Sano T, Nashimoto A, Kurita A, et al. Identification of risk factors for the development of complications following extended and superextended lymphadenectomies for gastric cancer. *Br J Surg.* 2005;92:1103–9.
28. Urien S, Lokiec F. Population pharmacokinetics of total and unbound plasma cisplatin in adult patients. *Br J Clin Pharmacol.* 2004;57:756–63.
29. Kohn R. Human aging and disease. *J Chronic Dis* 1963;16:5–21.
30. Bonenkamp JJ, Songun I, Hermans J, eSasako M, Welvaart K, Plukker JT, et al. Randomised comparison of morbidity after D1 and D2 dissection for gastric cancer in 996 Dutch patients. *Lancet.* 1995;345:745–8.
31. Tsujinaka T, Sasako M, Yamamoto S, Sano T, Kurokawa Y, Nashimoto A, Kurita A, Katai H, Shimizu T, Furukawa H, Inoue S, Hiratsuka M, Kinoshita T, Arai K, Yamamura Y; Gastric Cancer Surgery Study Group of Japan Clinical Oncology Group. Influence of overweight on surgical complications for gastric cancer: results from a randomized control trial comparing D2 and extended para-aortic D3 lymphadenectomy (JCOG9501). *Ann Surg Oncol.* 2007;14(2):355–61.

Gastric Cancer
DOI 10.1007/s10120-014-0365-z

ORIGINAL ARTICLE

Skeletal muscle loss after total gastrectomy, exacerbated by adjuvant chemotherapy

Yusuke Yamaoka · Kazumasa Fujitani · Toshimasa Tsujinaka · Kazuyoshi Yamamoto · Motohiro Hirao · Mitsugu Sekimoto

Received: 7 November 2013 / Accepted: 28 February 2014

Abstract
Background Skeletal muscle loss is associated with physical disability, nosocomial infections, postoperative complications, and decreased survival. Preventing the loss of skeletal muscle mass after gastrectomy may lead to improved outcomes. The aims of this study were to assess changes in skeletal muscle mass after total gastrectomy (TG) and to clarify the clinical factors affecting significant loss of skeletal muscle after TG.
Patients and methods One hundred and two patients undergoing TG for primary gastric cancer underwent abdominal computed tomography before and 1 year after TG to precisely quantify postoperative changes in skeletal muscle and adipose tissue. Univariate and multivariate logistic regression analyses identified clinical factors contributing to significant loss of skeletal muscle after TG.
Results At 1 year after TG, the mass of both skeletal muscle and adipose tissue was reduced by 6.20 ± 6.80 and 65.8 ± 36.1 % of the preoperative values, respectively, and 26 patients (25.5 %) showed a significant loss of skeletal muscle of more than 10 %. Adjuvant chemotherapy with S-1 for ≥6 months (hazard ratio 26.61, 95 % confidence interval, 3.487–203.1) was identified as the single independent risk factor for a significant loss of skeletal muscle.
Conclusions Skeletal muscle loss was exacerbated by extended adjuvant chemotherapy after TG. Further research should identify appropriate nutritional interventions for maintaining skeletal muscle mass and leading to improved outcomes.

Keywords Total gastrectomy · Skeletal muscle loss · Adjuvant chemotherapy · S-1 · Risk factor

Introduction

Skeletal muscle loss is associated with aging and physical disability [1] and is also caused by chronic disease and malignancy [2]. It leads to nosocomial infections [3], postoperative complications [4–7], increased length of hospital stay [7, 8], and decreased survival in nonmalignant as well as malignant populations [9–12].

Body weight loss is common in patients with gastric cancer undergoing total gastrectomy (TG). Although the main postoperative change in body composition after TG is a loss of fat mass, various degrees of skeletal muscle mass reduction have been demonstrated [13–15]. Preventing the loss of skeletal muscle mass after TG may lead to improved outcomes.

This retrospective analysis was conducted to reveal changes in body composition, including skeletal muscle mass, that occur after TG, and to clarify clinical factors affecting significant loss of skeletal muscle.

Y. Yamaoka · K. Yamamoto · M. Hirao · M. Sekimoto
Department of Surgery, National Hospital Organization Osaka National Hospital, Osaka, Japan
e-mail: yamaoka.yusuke@gmail.com

K. Fujitani (✉)
Department of Surgery, Osaka Prefectural General Medical Center, 3-1-56 Bandaihigashi, Sumiyoshi-ku, Osaka 558-8558, Japan
e-mail: fujitani@gh.opho.jp

T. Tsujinaka
Department of Surgery, Kaizuka City Hospital, Kaizuka, Japan

Published online: 09 April 2014

Patients and methods

Study population

We retrospectively reviewed the records of 218 patients who had undergone TG for primary gastric cancer between January 1, 2006 and December 31, 2011 at Osaka National Hospital. Patients with preoperative chemotherapy ($n = 47$), any incurable factors ($n = 37$), relapse within 1 year after surgery ($n = 24$), or concurrent malignancy ($n = 8$) were excluded from this analysis. The remaining 102 patients served as our study cohort. All the patients underwent open TG with Roux-en-Y reconstruction, and those with pathological stage II/III disease according to the Japanese classification of gastric carcinoma [16] received postoperative adjuvant chemotherapy with the oral 5-fluorouracil (5-FU) agent S-1 for 1 year if tolerated.

Data were collected on the following variables: age, sex, preoperative body mass index (BMI), the presence of diabetes mellitus (DM) requiring medications or insulin therapy, surgical procedures (degree of lymph node dissection and presence of combined splenectomy and/or distal pancreatectomy), postoperative complications according to the Clavien–Dindo classification [17], pathological stage, and compliance with adjuvant chemotherapy.

CT image analysis of body composition

Abdominal computed tomography (CT) images were acquired both preoperatively and at 1 year (median, 1.0 year; range, 0.90–1.10 years) postoperatively in all patients for the evaluation of tumor staging and diagnosis of recurrent disease. CT imaging also provided a means of precisely quantifying body composition [18]. CT images at the third lumbar vertebra (L3) were assessed for each patient. Images were analyzed with Volume Analyzer SYNAPSE VINCENT (Fujifilm, Tokyo, Japan), which enabled the demarcation of specific tissues using Hounsfield units (HUs). Skeletal muscle was identified and quantified by HU thresholds of −29 to 150 [19]. The muscles in the L3 region are the psoas, erector spinae, quadratus lumborum, transversus abdominis, external and internal obliques, and rectus abdominis. The following HU thresholds were used for adipose tissues: −190 to −30 for subcutaneous and intramuscular adipose tissue [20], and −150 to −50 for visceral adipose tissue [21]. Tissue boundaries were manually corrected if needed. Tissue cross-sectional area (cm^2) was calculated automatically by summing tissue pixels and multiplying by pixel surface area, and was subsequently normalized for stature (m^2) and reported as lumbar skeletal muscle index (SMI) (cm^2/m^2) and adipose tissue index (ATI) (cm^2/m^2) [18]. All CT images were analyzed by a single trained specialist. Postoperative changes in skeletal muscle and adipose tissue were evaluated.

Statistical analysis

SAS statistical software version 5.0 (SAS Institute, Cary, NC, USA) was used for all statistical analyses, and a P value <0.05 was considered significant. Data are presented as mean ± SD. The two-sample independent t test and χ^2 test were employed to evaluate differences in continuous and categorical variables, respectively. Univariate and multivariate logistic regression analyses were used to identify clinical risk factors for a significant loss of skeletal muscle mass after TG.

Results

Patient characteristics

The clinical characteristics of the 102 patients are listed in Table 1. No patients showed recurrence at the evaluation of body composition. The study population consisted of 71 men and 31 women with a mean age of 63.9 ± 10.5 years.

Table 1 Patient characteristics ($n = 102$)

Characteristic	$n = 102$
Age (years)	63.9 ± 10.5
Sex	
Male	71
Female	31
Preoperative body mass index (kg/m^2)	22.6 ± 3.25
Diabetes mellitus	
Present	9
Absent	93
Surgical procedure	
Lymphadenectomy D1+/D2	10/92
Splenectomy/distal pancreatectomy	16/2
Postoperative complication	22
Anastomotic leakage	3
Pancreatic fistula	5
Intraabdominal abscess	7
Ileus	1
Wound dehiscence	4
Pneumonia	2
Clavien–Dindo classification of postoperative complications	
Grade II/III/IV	14/7/1
Pathological stage I/II/III	50/28/24
Adjuvant chemotherapy	
None or <6 months	64
≥6 months	38

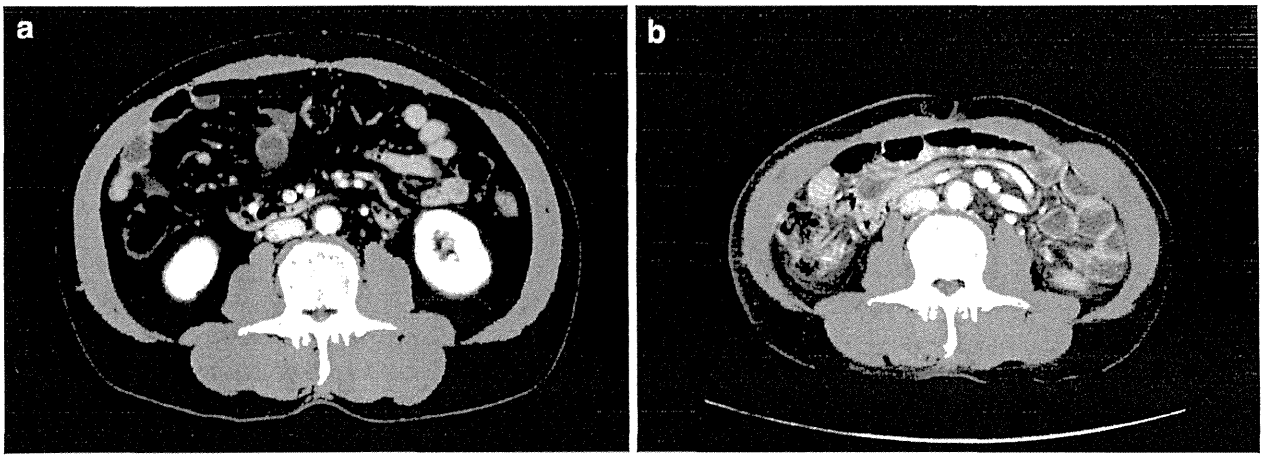

Fig. 1 Typical transverse computed tomography (CT) images at L3 show postoperative changes in skeletal muscle (*green*). The preoperative total muscle area of 143 cm^2 (**a**) decreased to 122 cm^2 at 1 year after surgery (**b**)

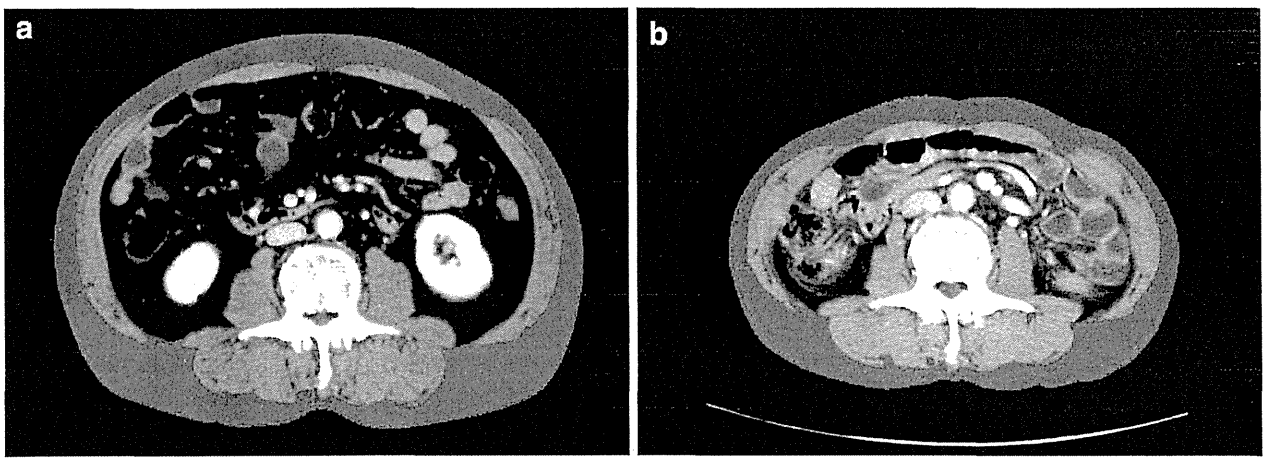

Fig. 2 Typical transverse CT images at L3 show postoperative changes in subcutaneous and intramuscular adipose tissue (*green*). The preoperative subcutaneous and intramuscular adipose tissue area of 135 cm^2 (**a**) decreased to 89 cm^2 at 1 year after surgery (**b**)

The preoperative mean BMI of all patients was 22.6 ± 3.25 kg/m^2. Nine patients had comorbid DM and none received steroid therapy. Ninety-two patients underwent D2 lymphadenectomy, with combined splenectomy and distal pancreatectomy performed in 16 and 2 patients, respectively. No patient underwent lower mediastinal dissection for esophageal invasion. Postoperative complications were observed in 22 patients, involving anastomotic leakage in 3, pancreatic fistula in 5, intraabdominal abscess in 7, ileus in 1, wound dehiscence in 4, and pneumonia in 2. Based on the Clavien–Dindo classification [17], these complications were categorized as grade II, III, and IV in 14, 7, and 1 patients, respectively. Fifty-two patients had pathological stage II/III disease, and of these, 38 tolerated adjuvant S-1 therapy for 6 months or more after surgery.

Postoperative changes in skeletal muscle and adipose tissue

Figure 1 shows typical transverse CT images at L3 featuring postoperative changes in skeletal muscle. The preoperative skeletal muscle area of 143 cm^2 (Fig. 1a) decreased to 122 cm^2 at 1 year after surgery (Fig. 1b); the preoperative SMI of 58.6 cm^2/m^2 (Fig. 1a) declined to 50.0 cm^2/m^2 (Fig. 1b). Similarly, Figs. 2 and 3 demonstrate typical transverse CT images at L3 showing postoperative changes, in subcutaneous plus intramuscular adipose tissue (Fig. 2) and in visceral adipose tissue (Fig. 3). The preoperative total adipose tissue area, which is the sum of subcutaneous, intramuscular, and visceral adipose tissues, decreased from 296 to 105 cm^2 at 1 year after surgery, and the preoperative ATI of 122 cm^2/m^2

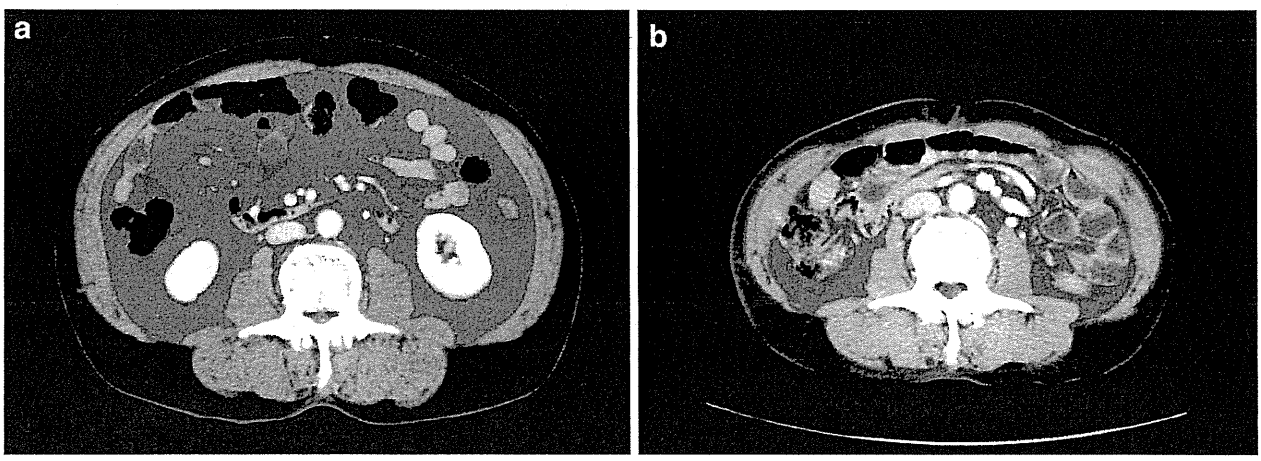

Fig. 3 Typical transverse CT images at L3 show postoperative changes in visceral adipose tissue (*green*). The preoperative visceral adipose tissue area of 161 cm^2 (**a**) decreased to 16 cm^2 at 1 year after surgery (**b**)

Table 2 Changes in body composition of patients undergoing total gastrectomy (TG) for gastric cancer ($n = 102$)

	Preoperative	1 year after TG	Percent decrease
Body mass index (BMI) (kg/m^2)	22.6 ± 3.25	19.1 ± 2.43	14.7 ± 8.37
Lumbar skeletal muscle index (SMI) (cm^2/m^2)	46.6 ± 7.84	43.6 ± 6.92	6.20 ± 6.80
Lumbar adipose tissue index (ATI) (cm^2/m^2)	76.4 ± 36.4	21.4 ± 18.9	65.8 ± 36.1

decreased to 43.1 cm^2/m^2. Postoperative changes in body composition are detailed in Table 2. At 1 year after surgery, mean BMI (kg/m^2) decreased from 22.6 to 19.1, SMI (cm^2/m^2) from 46.6 to 43.6, and ATI (cm^2/m^2) from 76.4 to 21.4, which corresponded to reductions of the preoperative values of 14.7 ± 8.37 %, 6.20 ± 6.80 %, and 65.8 ± 36.1 %, respectively.

Risk factors for significant postoperative loss of skeletal muscle

Twenty-six patients (25.5 %) showed a significant loss of skeletal muscle of more than 10 % at 1 year after TG. Table 3 summarizes the results of univariate and multivariate analyses of various clinicopathological risk factors for a significant loss of skeletal muscle, including age, sex, presence of DM, postoperative complications according to the Clavien–Dindo classification, pathological stage, compliance with adjuvant chemotherapy (none or <6 months versus ≥6 months), and preoperative SMI and ATI. Among these, adjuvant chemotherapy lasting for ≥6 months (hazard ratio, 26.61; 95 % confidence interval, 3.487–203.1) was identified as the single independent risk factor for a significant loss of skeletal muscle after TG. In addition, we compared the change of body composition after TG between patients who received adjuvant S-1 chemotherapy (≥6 months) and those who did not (Table 4). There was no significant difference in terms of decreased body weight or ATI, whereas SMI decreased significantly in patients receiving adjuvant chemotherapy ($P < 0.001$).

Discussion

We conducted specific quantification of skeletal muscle mass by CT image analysis in patients undergoing TG. Using this approach, we demonstrated the postoperative changes in skeletal muscle mass and adipose tissue and identified the clinical factors contributing to a significant loss of skeletal muscle mass after TG. CT scan is the gold standard for quantifying skeletal muscle mass [22], and Mourtzakis et al. [18] have shown that the CT cross sectional area at L3 is strongly related to appendicular skeletal mass, a common index of sarcopenia as measured by dual-energy X-ray densitometry. CT cross-sectional area at L3 single slice was employed in many studies as a reliable method to evaluate body composition [7, 10, 23].

In our study, mean SMI (cm^2/m^2) decreased from 46.6 to 43.6 by 1 year after surgery and ATI (cm^2/m^2) decreased from 76.4 to 21.4; these declines corresponded to 6.2 % and 65.8 % reductions of the preoperative values, respectively (Table 2). The general extent to which skeletal muscle mass decreases after gastrectomy remains unclear because few body composition studies have been conducted, and no research before our own has used CT image analysis to evaluate changes in skeletal muscle mass